Journal of the Korean Nuclear Society
Volume 28, Number 2, April 1996

A Deformation Model of Uranium-Silicide Dispersion Fuel for Research Reactor

T.S. Byun, S.K. Suh, and W. Hwang
Korea Atomic Energy Research Institute
(Received October 4, 1995)

연구로용 우라늄-실리사이드 분산 핵연료의 변형모델

변택상 · 서성기 · 황 완
한국원자력연구소
(1995. 10. 4 접수)

Abstract

A deformation model was developed to calculate the deformation of the uranium-silicide dispersion fuel (U_3Si-Al) elements for research reactors. The model was based on the elasto-plasticity theory and power-law creep theory. Also, isotropic swelling was assumed for the fuel meat and isotropic thermal expansion for the fuel meat and cladding. The new model calculated successfully the deformation of the fuels of HANARO and NRU (in Canada). As the most important result, it was shown that the primary deformation mechanism in the fuel meat was swelling and that in the cladding was creep. For all cases simulated, the maximum hoop stress at cladding outer surface was less than 5 MPa, probably well below the yield stress of the cladding, and finally, the volume change was predicted to be less than 10% in the whole burnup range.

요 약

연구로용 우라늄-실리사이드 분산 핵연료에서의 응력 및 변형율 분포를 계산할 수 있는 변형모델을 개발하였다. 이 변형모델은 탄소성이론 및 지수법칙 크리프이론을 기초로 한 것이며, 또한 등방 핵연료팽윤 및 열팽창을 가정하였다. 개발된 모델을 HANARO 및 카나다의 NRU 핵연료에 적용하여 본 결과 핵연료의 변형을 성공적으로 계산하는 것으로 판단되었다. 계산결과에 따르면, 연구로용 우라늄-실리사이드 분산핵연료가 연소할 때 핵연료심에서 가장 중요한 변형기구는 팽윤이며, 피복관에서 가장 중요한 변형기구는 크리프이다. 또한, 피복관에서 원주방향 최대응력은 항상 5 MPa 이하로서 항복응력보다 훨씬 낮게 유지되었다. 여기서 고려한 두 핵연료설계에 대해서 전 연소도 범위에서 핵연료봉의 부피변화는 10% 이하로 예측되었다.

1. Introduction

Uranium-silicide dispersion fuel (U_3Si-Al) with low-enriched uranium of about 20 wt.% U-235 has been developed and used in research reactors, and one type of the fuel is being developed for the HANARO[1-3]. The meat (or core) of the fuel is a composite of uranium-silicide(U_3Si) particles and alumi-

num(Al) matrix, and is metallurgically extrusion-bonded with Al-1060 cladding. Spherical U_3Si particles of about 22% volume fraction are dispersed in a continuous Al matrix[3].

In the uranium-silicide dispersion fuel, the most important driving force for deformation is believed to be fuel meat swelling[4]. When compared to the commercial UO_2 fuels, the discharge burnup is very high (up to about 20000 MWh/kgU), therefore, the fuel swelling can also be high enough to cause large permanent plastic deformation. The fuel swelling occurs due to formation of fission gas bubbles, accumulation of solid fission products, and formation of an interfacial layer (uranium-aluminides) having lower density.

Thermal calculations[3] showed that the fuel temperatures were in the range of 400-500 K for a typical equilibrium core. Aluminum alloys have a relatively low melting point of about 920 K[5], and the creep deformation usually becomes important when the temperature is above one half of the melting point, so the creep rate, in the aluminum matrix as well as in the Al-1060 cladding, will be very high in the fuel operating temperature range. Creep deformation can easily relax the stresses within the fuel element, and therefore the deformation of cladding can be characterized by a 'low-stress and creep-dominant deformation'. A special deformation model is needed to predict the characteristic deformation behaviour of the research reactor fuels.

The objective of this study is to develop a deformation model to predict the distributions of strain and stress within the U_3S_i-Al fuel element. In the present study, the fuel element is modelled as a circular composite beam composed of fuel core(meat) and cladding. The variations of strain and stress are described by one dimensional (radial) finite difference method. Creep rates of fuel meat and cladding are calculated on the basis of the dislocation creep theory and experimental results[6, 7]. Other relationships and theories applied to this modelling are [8-10] : the force equilibrium equation, compatibility equation for strains (strain rates), stress-strain relationships (constitutive equations) based on the total strain theory, power-law strain hardening for plastic deformation, and constant volume condition for pure plastic deformation. Isotropic fuel swelling and thermal expansion are also assumed.

The fuel element was regarded as a continuum, thus no interfacial gap was modelled between fuel meat and cladding. So the boundary conditions applied are[8] : (a) the radial stress is continuous at the meat/cladding interface, (b) the hoop strain (or radial displacement) and hoop strain rate are continuous at the meat/cladding interface, (c) the radial stress at cladding outer surface is the same as the value of $(-1)\times$coolant pressure, and (d) the gradients of stresses and strains are zero at fuel center.

The deformation model newly developed was named as STRESS and integrated into the DIFAIR code [3, 4]. The DIFAIR code has been developed to analyze research reactor fuel performance under normal and off-normal operation conditions.

This paper describes the deformation model developed, and discusses the characteristic stress and strain distributions in the uranium-silicide dispersion fuels for research reactor. Additionally, the calculation results, volume changes, are compared with the results of the FZZ-918 experiment done by CRNL [1, 2].

2. Modelling of Fuel Element Deformation

The schematic cross-sectional view of fuel element is shown in Fig. 1, and the system is assumed to be axisymmetric. The cylindrical coordinate system (r, θ, z), where r, θ, z are radial, tangential, and axial directions, respectively, is used in this fuel modelling. However, since this model is an one-dimensional model, no variable has tangential or axial variation. Also, since the fuel meat-cladding composite is assumed to be a continuum, the radial gap between fuel meat and cladding is always closed, and no central void can form during irradiation. The fuel meat and cladding are divided into multiple annuli, typically 50 an-

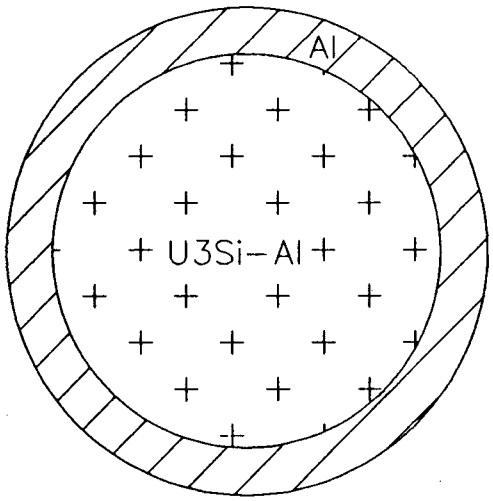

Fig. 1. Schematic Diagram of Uranium-Silicide Dispersion Fuel

nuli, to formulate the finite difference equations for governing equations.

2.1. Strain Rate Distribution

Since the fuel element considered in this modelling is assumed as a continuum, the deformation have to obey the compatibility equations. In the cylindrical coordinate system (r, θ, z), the compatibility equation is given by[8, 10]

$$\frac{d\varepsilon_\theta}{dr} + \frac{\varepsilon_\theta - \varepsilon_r}{r} = 0 \tag{1}$$

where ε_θ and ε_r are hoop strain and radial strain, respectively, and r is the radial position. Differentiating the strain components with time(t), the strain rate components labeled $\dot{\varepsilon}_\theta$ and $\dot{\varepsilon}_r$ also satisfy the same form of compatibility equation. That is

$$\frac{d\dot{\varepsilon}_\theta}{dr} + \frac{\dot{\varepsilon}_\theta - \dot{\varepsilon}_r}{r} = 0 \tag{2}$$

The two terms of this equation are, respectively, approximated as follows:

$$\frac{d\dot{\varepsilon}_\theta}{dr} = \frac{\dot{\varepsilon}_\theta^{i+1} - \dot{\varepsilon}_\theta^{i}}{r^{i+1} - r^{i}} \tag{3a}$$

$$\frac{\dot{\varepsilon}_\theta - \dot{\varepsilon}_r}{r} = \frac{1}{2}\left(\frac{\dot{\varepsilon}_\theta^{i+1} - \dot{\varepsilon}_r^{i+1}}{r^{i+1}} + \frac{\dot{\varepsilon}_\theta^{i} - \dot{\varepsilon}_r^{i}}{r^{i}}\right) \tag{3b}$$

where the superscripts i and i+1 mean the numbers of ith and (i+1)th annuli of radially-segmented fuel. Replacing the two terms in equation (2) with these two equations, then the equation (2) becomes

$$p\,\dot{\varepsilon}_\theta^{i+1} + q\,\dot{\varepsilon}_r^{i+1} = h_\varepsilon \tag{4}$$

where

$$p = \frac{1}{r^{i+1} - r^{i}} + \frac{1}{2r^{i+1}}$$

$$q = -\frac{1}{2r^{i+1}}$$

$$h_\varepsilon = \frac{\dot{\varepsilon}_\theta^{i}}{r^{i+1} - r^{i}} - \frac{\dot{\varepsilon}_\theta^{i} - \dot{\varepsilon}_r^{i}}{2r^{i}}$$

Since isotropic fuel core swelling and isotropic thermal expansion are assumed, the strain rate components can be expressed as

$$\dot{\varepsilon}_r = \dot{\varepsilon}^{th} + \dot{\varepsilon}^{s} + \dot{\varepsilon}_r^{c} \tag{5a}$$

$$\dot{\varepsilon}_\theta = \dot{\varepsilon}^{th} + \dot{\varepsilon}^{s} + \dot{\varepsilon}_\theta^{c} \tag{5b}$$

where $\dot{\varepsilon}^{th}$ is thermal expansion strain rate, $\dot{\varepsilon}^{s}$ swelling strain rate, and $\dot{\varepsilon}_r^{c}$ and $\dot{\varepsilon}_\theta^{c}$ creep strain rate components.

Creep deformation and instantaneous plastic deformation occur under constant volume condition (unlike elastic deformation, swelling, or thermal expansion). The present model assumes that creep does not occur along the axis direction (z-direction); $\dot{\varepsilon}_z^{c}=0$. So the components of creep strain are related by the constant volume condition : $\dot{\varepsilon}_r^{c}+\dot{\varepsilon}_\theta^{c}=0$.

Using this constant volume condition and equations (4), (5a), and (5b), the θ−components of creep strain rate at (i+1)th annulus can be expressed as

$$\dot{\varepsilon}_{\theta}^{c,i+1} = \frac{h_{\varepsilon} - (p+q)(\dot{\varepsilon}_{r}^{th,i+1} + \dot{\varepsilon}_{r}^{s,i+1})}{(p-q)} \quad (6)$$

With the constant volume condition, the radial component of creep strain rate at (i+1)th annulus is given by

$$\dot{\varepsilon}_{r}^{c,i+1} = -\dot{\varepsilon}_{\theta}^{c,i+1} \quad (7)$$

Each total strain rate component is the sum of thermal strain rate, swelling strain rate, and creep strain rate. These strain rates have to be evaluated by separate models. First, the thermal strain rate ($\dot{\varepsilon}^{th}$) is calculated under the assumption of isotropic thermal expansions. Also, the thermal expansion coefficients are assumed to be constant for the fuel temperature range of research reactors. The thermal expansion coefficients used are given by $\alpha_{Al}=24.6\times10^{-6}$ [1/K] for Al, and $\alpha_{U_3Si}=14.2\times10^{-6}$ [1/K] for U_3Si[3]. Here, the thermal expansion coefficient of fuel meat (U_3Si-Al) with about 22 vol.% U_3Si particles is calculated to be $\alpha_{U_3Si-Al}=22.0\times10^{-6}$ [1/K] by mixture rule. Then, the thermal expansion strain rates at fuel meat and cladding are, respectively, given by

$$\dot{\varepsilon}^{th} = \alpha_{U_3Si-Al}\dot{T} \quad \text{at fuel meat} \quad (8a)$$

$$\dot{\varepsilon}^{th} = \alpha_{Al}\dot{T} \quad \text{at cladding} \quad (8b)$$

where $\dot{T}$ is the temperature change rate at the position.

Secondly, the swelling strain rate, $\dot{\varepsilon}^{s}$, is evaluated by a fuel swelling model[4], in which the swelling of the silicide fuel comprises three major components: (a) volume change due to thermal-chemical reactions at the interfaces of uranium-silicide fuel particles and aluminum matrix, (b) volume change due to nucleation and growth, and coalescence of fission gas bubbles, and (c) volume change due to solid fission products and due to phase change by depletion of uranium in U_3Si compound.

Thirdly, the creep strain rate components, $\dot{\varepsilon}_{r}^{c}$, $\dot{\varepsilon}_{\theta}^{c}$, are evaluated on the basis of a dislocation creep model and experimental data for aluminum[7]. In the equilibrium core, the power and burnup would vary at a low rate and fuel core swelling and thermal expansion, which cause the creep deformation, occur at nearly constant rate for a small burnup interval. Consequently, the creep deformation occurs in the regime of secondary creep in which the creep strain rate is almost constant for given temperature and stress. We determined the dislocation creep mechanism (m=4.5 in the following equation) as the major mechanism of creep deformation for the stress level of fuel element of research reactor (see Fig. 8 and 9). The equivalent strain rate is expressed as a power-law creep equation[6, 9]:

$$\dot{\varepsilon}^{c} = A\sigma^{m}e^{-Q_c/RT} \quad (9)$$

where A is a constant ($=5.8\times10^{7}$ for Al), R is the gas constant ($=1.98$ cal/mol. K), σ is equivalent stress, m is the stress exponent in the power-law creep ($=4.5$), and Q_C activation energy for creep ($=30$ kcal/mole at around 400 K)[6].

With the constant volume condition ($\dot{\varepsilon}_{r}^{c}+\dot{\varepsilon}_{\theta}^{c}=0$) and with the assumption of $\dot{\varepsilon}_{z}^{c}=0$, the equivalent plastic strain rate is given by[8, 10]

$$\dot{\varepsilon}^{c} = \frac{\sqrt{2}}{3}[(\dot{\varepsilon}_{r}^{c}-\dot{\varepsilon}_{\theta}^{c})^2+(\dot{\varepsilon}_{\theta}^{c})^2 + (\dot{\varepsilon}_{r}^{c})^2]^{1/2} = \frac{2}{\sqrt{3}}\dot{\varepsilon}_{\theta}^{c} \quad (10)$$

2.2. Stress Distribution

In the cylindrical coordinate system (r, θ, z), the force equilibrium conditions[8, 10] become a governing equation for stress distribution by eliminating shear stresses and θ- and z-derivatives:

$$\frac{d\sigma_r}{dr} + \frac{\sigma_r - \sigma_\theta}{r} = 0 \quad (11)$$

For formulation of finite difference equation, the first term and second term are approximated by

$$\frac{d\sigma_r}{dr} = \frac{\sigma_r^{i+1} - \sigma_r^{i}}{r^{i+1} - r^{i}} \quad (12a)$$

$$\frac{\sigma_r - \sigma_\theta}{r} = \frac{1}{2}\left(\frac{\sigma_r^{i+1} - \sigma_\theta^{i+1}}{r^{i+1}} + \frac{\sigma_r^{i} - \sigma_\theta^{i}}{r^{i}}\right) \quad (12b)$$

Regarding that the stress components of the ith annulus, σ_r^i and σ_θ^i, and radial position, r^i and r^{i+1}, are known, the above equation can become a relationship for σ_r^{i+1} and σ_θ^{i+1}:

$$p\sigma_r^{i+1} + q\sigma_\theta^{i+1} = h_\sigma \quad (13)$$

where p and q are defined in equation (4), and

$$h_\sigma = \frac{\sigma_r^i}{r^{i+1} - r^i} - \frac{\sigma_r^i - \sigma_\theta^i}{2r^i}$$

Since two dimensional deformation in the r-θ plane is assumed, the stress components are related by Tresca equation[9, 10]; $\sigma = \sigma_\theta - \sigma_r$, where σ is the equivalent stress. At each annulus, the equivalent stress can be evaluated by the creep rate equation (9). Inserting the Tresca equation into equation (13), the hoop stress at (i+1)th annulus can be expressed by

$$\sigma_\theta^{i+1} = \frac{h_\sigma + p\sigma^{i+1}}{(p+q)} \quad (14)$$

From the Tresca equation, then, the radial stress at (i+1)th annulus is given by

$$\sigma_r^{i+1} = \sigma_\theta^{i+1} - \sigma^{i+1} \quad (15)$$

2.3. Total Strain

Total strain components are obtained using the constitutive equations. Each strain component comprises five strain terms. Letting ε_r and ε_θ be the total strain components in the radial and hoop directions, the constitutive equations are expressed by[8]

$$\varepsilon_r = A\sigma_r - B(\sigma_\theta + \sigma_z) + \varepsilon^{th} + \varepsilon^s + \varepsilon_r^c \quad (16a)$$

$$\varepsilon_\theta = A\sigma_\theta - B(\sigma_z + \sigma_r) + \varepsilon^{th} + \varepsilon^s + \varepsilon_\theta^c \quad (16b)$$

where ε^{th} is the strain due to isotropic thermal expansion, ε^s the swelling strain component, and ε_r^c and ε_θ^c the creep strain components. These three kinds of strains are obtained by summation of the strain increments ($\varepsilon \Delta t$) of respective time (burnup) intervals. Further, on the basis of general linear elasticity and Hencky's total strain theory[10], the coefficient A and B (and H) are given by

$$A = \frac{1}{E} + \frac{2}{3}H \quad (17a)$$

$$B = \frac{\nu}{E} + \frac{1}{3}H \quad (17b)$$

$$H = \frac{3}{2}\frac{\varepsilon^p}{\sigma} = \frac{3}{2}\frac{(\sigma/K)^{1/n}}{n\sigma} \quad (17c)$$

Here, E is the Young's modulus (88.6 GPa for fuel meat and 70 GPa for cladding), ν is Poisson ratio (0.3 for fuel meat and 0.33 for cladding). Power-law hardening is assumed for stress-plastic strain relationship; $\sigma = K(\varepsilon^p)^n$, here ε^p is the instantaneous equivalent plastic strain, K is the strength coefficient (100 for both fuel meat and cladding), and n is the strain hardening coefficient (0.2 for both fuel meat and cladding).

If using the strains calculated by above equations (16a) and (16b), the radial displacement(U) at each annulus and element volume change can be evaluated. The radial displacement and hoop strain are related by an equation of $U = \varepsilon_\theta / r$. The element volume change, in %, is defined by $100 \times ((r_0 + U_0)^2 - r_0^2)/r_0^2$, where r_0 is the outer radius of cladding before deformation, and U_0 is the displacement at cladding outer surface.

2.4. Boundary Conditions

At the center of fuel element (r=0) no variable can have radial gradient. This condition can be applied to strain rate and stress distributions; $d\dot{\varepsilon}_\theta/dr = 0$ and $d\sigma\theta/dr = \dot{0}$. Applying these conditions to the compatibility equation (2) and force equilibrium equation (11), and considering the fact that the second terms of right hand side of these equations become infinity when r goes to zero, the stress and

strain components have to satisfy the following relationships :

$$\dot{\varepsilon}_r = \dot{\varepsilon}_\theta \tag{18a}$$

$$\sigma_r = \sigma_\theta \tag{18b}$$

At the interface between fuel meat and cladding the following conditions can be derived from the continuity condition of displacement and force :

$$\dot{\varepsilon}_\theta^{meat} = \dot{\varepsilon}_\theta^{clad} \tag{19a}$$

$$\sigma_r^{meat} = \sigma_r^{clad} \tag{19b}$$

At fuel element surface the boundary condition applied is that the radial stress is balanced with the coolant pressure (P_c =0.3 MPa), that is

$$\sigma_r = -P_c \tag{20}$$

This boundary condition will be used as the criterion for the convergence of solution in iterative calculation.

2.5. Numerical Scheme

The calculation procedure of the STRESS model is illustrated as a flow chart in Fig. 2. Temperature distribution, total swelling strain distribution, radial positions of nodes, etc are given from other subroutines in DIFAIR code. From these input data the swelling strain rate and thermal strain rate are calculated for each node of annulus. The strain rates are assumed to be constant for the time interval (given in hour) that is calculated from the element power and burnup increment.

The first step of iterative calculation is to assume a value of radial stress at fuel center (i = 1). Until the radial stress at cladding surface converges to the value of $-P_c$ (P_c = coolant pressure ; 0.3 MPa), re-assumption of a radial stress value at fuel center and subsequent calculations are repeated. Iterative calculation would be stopped if the calculated radial stress at cladding surface satisfies the convergence criterion ; | radial stress at cladding surface + coolant pressure | ≤ 0.02 MPa. Detailed calculation methods were explained in the previous sections 2.1 to 2.4.

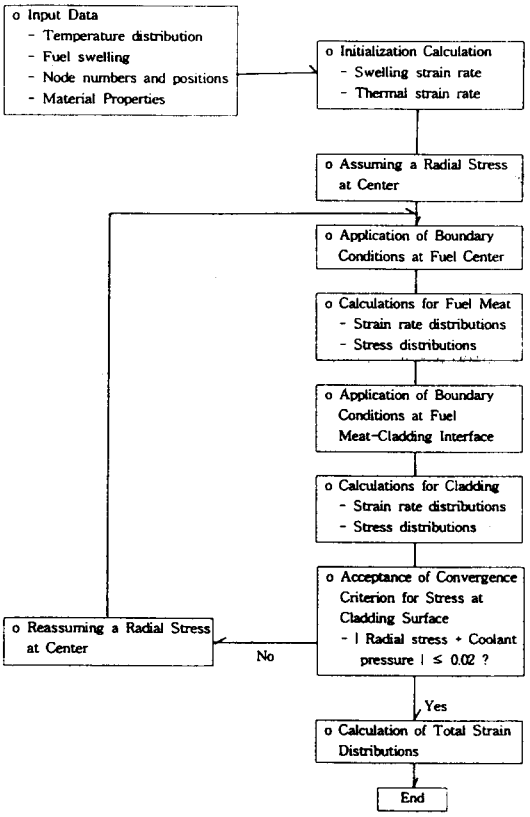

Fig. 2. Calculational Procedure of STRESS Program

3. Application and Results

3.1. Input Data and Case Descriptions

Deformation behaviors of two uranium-silicide dispersion fuels were simulated with the newly-developed deformation model, STRESS. The two fuels simulated are a HANARO fuel element and a NRU fuel element. The input parameters of DIFAIR code for the two uranium-silicide fuels are listed in Table 1(note that the effect of fins are not considered in this model). As seen in this table, the most important difference between these two fuels is on the radius of fuel meat.

The present sample calculations use a typical el-

ement burnup-power history given in Table 2. Total 8 cases (1 case for HANARO fuel and 7 cases for NRU fuel) were simulated, as summarized in Table 3. The 7 cases for NRU fuel element are to simulate the experiment done by CRNL, named as FZZ-918 [1, 2].

Deformation characteristics of the uranium-silicide dispersion fuels will be discussed in detail by using the results for HANARO fuel element. The calculated results for the NRU fuel elements will be used to compare with the volume changes measured in the experiment FZZ-918.

3.2. Strain and Strain Rate Distribution

Fig. 3 illustrates the distributions of radial strain (ε_r) and hoop strain (ε_θ) within the fuel element at the burnup of 40 at.% (about 9000 MWh/kgU), at which the element power is peak power of 102 kW/m. Both strain components are almost constant in the fuel meat (note that the radius of fuel meat 3. 18mm). The distribution of hoop strain is continuous at meat-cladding interface, but distribution of radial strain is discontinuous. At cladding, the region that the distance from center is from 3.18mm to 3.94mm,

Table 1. Input Data for HANARO Fuel Element (36-Element Fuel) and NRU Fuel Element (Experiment FZZ-918)

Fuel Meat Data		
Diameter of fuel meat	=6.35 (5.5)	(mm)
Length of fuel element	=700.0	(mm)
Enrichment of fuel	=20.	(%)
Density of meat	$=0.53\times10^4$	(kg/m^3)
Density of uranium	$=0.31\times10^4$	(kg/m^3)
Weight fraction of U_3Si	=0.61	
Weight fraction of Al	=0.39	
Density of U_3Si	$=0.1558\times10^5$	(kg/m^3)
U_3Si particle size	=130 (70, 130)	(μm)
Surface tension	$=0.225\times10^{-3}$	(kJ/m^2)
Young's modulus of meat	$=0.886\times10^5$	(MPa)
Poisson's ratio of meat	=0.3	
Thermal expansion coe. of meat	$=0.22\times10^{-4}$	(1/K)
Thermal conductivity of meat	=0.16284	(kW/m. K)
Fuel Cladding and Fin Data		
Diameter of fuel cladding	=7.87 (7.02)	(mm)
Cladding thickness	=0.76	(mm)
Density of aluminum	$=0.27\times10^4$ (kg/m^3)	
Number of fins	=8	
Fin height	=1.02	(mm)
Fin width	=0.76	(mm)
Young's modulus of cladding	$=0.7\times10^5$	(MPa)
Poisson's ratio of cladding	=0.33	
Thermal expansion coefficient of cladding	$=0.246\times10^{-4}$	(1/K)
Thermal conductivity of cladding	=0.2168	(kW/m. K)
Thermal conductivity of crud and oxide layer	$=0.225\times10^{-2}$	(kW/m. K)

Note : The values in ( ) are the input data for NRU fuel element

Table 2. Burnup-power History

Burnup (at. %)	Power (kW/m)
25.0	95.2
40.0	102.0
58.2	88.0
60.0	82.7
79.0	82.7
82.0	34.7
94.0	34.7

Table 3. Case Descriptions

Case No.	Fuel Type	Final Burnup [at. %]	Element Diameter [mm]	U_3Si Particle Size [μm]
1	HANARO Fuel	94	7.87	130
2	NRU Fuel	40	7.02	130
3	NRU Fuel	62	7.02	130
4	NRU Fuel	82	7.02	130
5	NRU Fuel	94	7.02	130
6	NRU Fuel	40	7.02	70
7	NRU Fuel	60	7.02	70
8	NRU Fuel	78	7.02	70

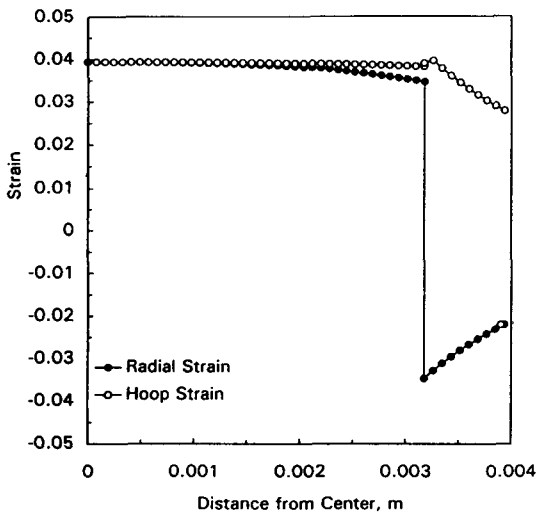

Fig. 3. Strain Distributions at the Burnup of 40 at.%

the hoop strain decreases with distance from center, whereas the radial strain increases with distance from center. Since plastic deformation at cladding would be subjected to the constant volume condition, the radial strain and hoop strain have reversed sign, but the absolute values of the two strain components are almost the same with each other.

These strain distributions can be explained by Fig. 4, in which the distributions of swelling strain, thermal strain, and creep strain are illustrated separately (since the elastic strain and instantaneous plastic strain are negligible, they are not treated in the present discussion). Comparing the strain components in Fig. 4, the deformation within the fuel meat is mainly due to the swelling, but the major deformation mechanism at cladding is the creep. The swelling strain is almost constant within fuel meat, and zero in the cladding made of aluminum alloy.

As seen in Fig. 4, the thermal strain is below 0.005 (0.5%) at fuel center and decreases with the distance from center. As mentioned in the section 2-1, the thermal expansion is proportional to the temperature change from the room temperature (293 K). Temperature distribution is shown in Fig. 5. Although the element linear power of 102 kW/m is the highest power in the power history given in Table 2, the temperatures that are proportional to the element power are only 410 K-490 K. This means that the tempera-

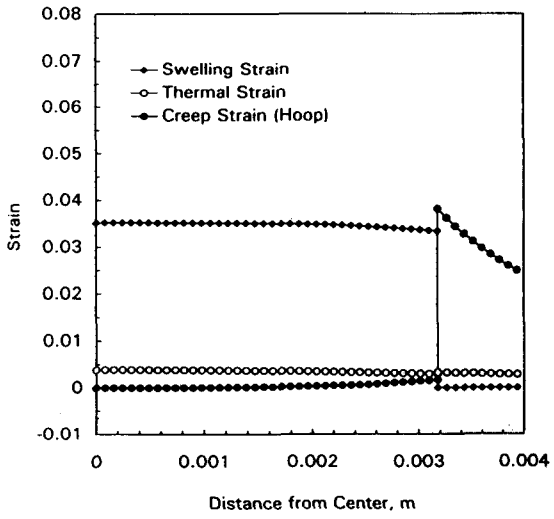

Fig. 4. The Distributions of Swelling, Thermal, and Creep Strains at the Burnup of 40 at.%

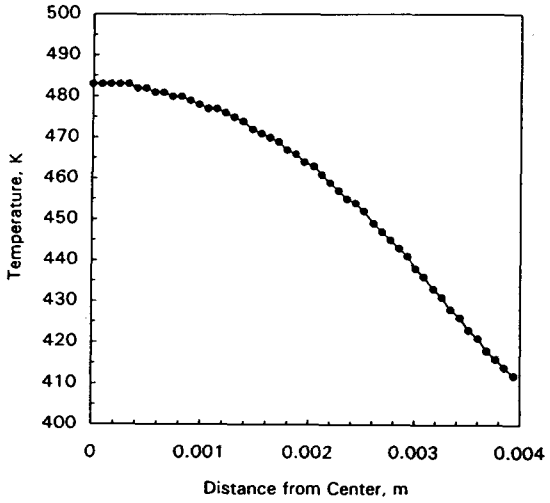

Fig. 5. Temperature Distribution at the Burnup of 40 at.%

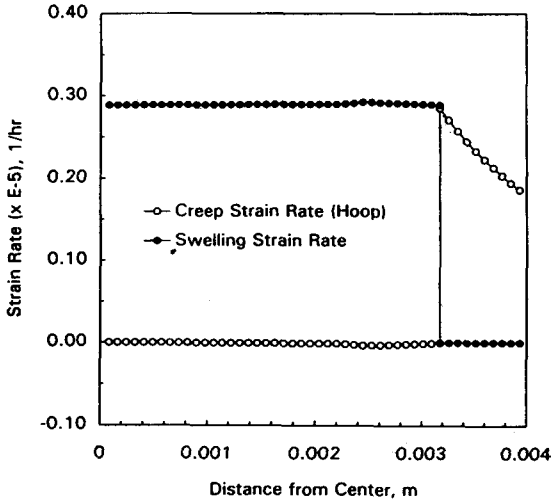

Fig. 6. Strain Rate Distributions at the Burnup of 40 at.%

ture change from the room temperature is less than 200K, which will produce about 0.5% strain. Therefore, it can be concluded that the thermal expansion is not major deformation mechanism in the uranium-silicide dispersion fuel.

Since in the present deformation model the stresses and strains are calculated based on the calculation of strain rates, a comparison of strain rates will directly explain the deformation characteristics. Fig. 6 compares the most important strain rates such as swelling strain rate and creep strain rate. Fig. 6 implies that almost uniform swelling occurs within the fuel meat at the swelling strain rate of 0.29×10^{-5} hr^{-1}. Creep strain rate in the hoop direction is almost zero at fuel meat, however, at meat-cladding interface it jumps up to the same value with the swelling strain of fuel meat, and then the creep strain rate decreases with the distance from center. Since the thermal strain rate is relatively small and the distribution is continuous at fuel meat-cladding interface, because the temperature distribution is continuous at the interface as seen in Fig. 5, the sum of the swelling strain rate and hoop creep strain rate have to be subjected to the condition of continuity at interface, as expressed by equation (19a).

In conclusion, the major deformation mechanisms of the uranium-sicilide dispersion fuel are the swelling of fuel meat and the creep of cladding. Through a mechanical interaction at fuel meat-cladding interface, most of the swelling strain of fuel meat is transformed into creep strain of cladding.

On the other hand, dimensional change is determined by the radial displacement(U). Fig. 7 shows the radial displacement versus position. Within the fuel meat the radial displacement almost linearly increases with the distance from center. This fact is coincided with the uniform swelling strain (or swelling strain rate) distribution. As discussed above, the cladding deformation is the creep deformation which is subjected to constant volume condition. This means that the cladding thickness would decrease as the meat swelling increases, although the radius of cladding increases. Thus the radial displacement decreases as the distance from center increases, and a peak displacement is founded at fuel meat-cladding interface. In Fig. 7 the radial displacement is about 0.11mm at cladding outer surface. About 5.67% volume change (expansion) is calculated from this value.

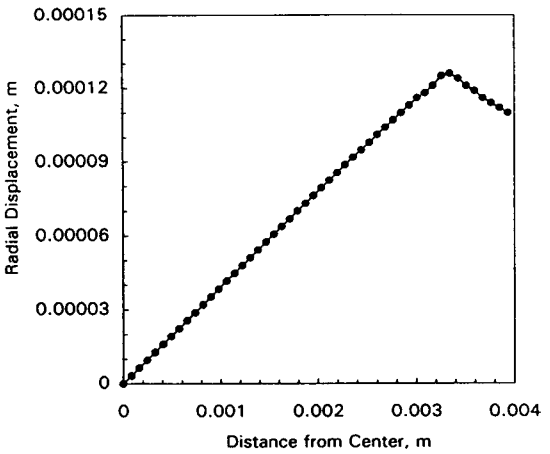

Fig. 7. Radial Displacement Versus the Distance From Fuel Center at the Burnup of 40 at.%

3.3. Stress Distribution

Fig. 8 illustrates the radial and hoop stress distributions. Both stress components increase with the distance from center, and have the same value at fuel center (r = 0). The hoop stress has a discontinuity at fuel meat-cladding interface. However, the radial stress is continuous through whole fuel element (the radial stress is subjected to the continuity condition at interface; see equation (19b)). The radial stress at cladding outer surface is the same with $-P_c$ (the coolant pressure) because of the boundary condition of equation (20).

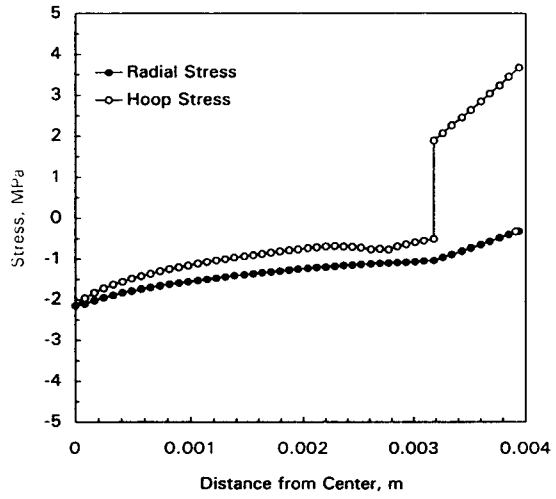

Fig. 8. Stress Distributions at the Burnup of 40 at.%

As seen in Fig. 8, the hoop stress is maximum at cladding outer surface and always positive (tensile) at cladding, however, the radial stress is always compressive at cladding. The maximum hoop stress predicted is about 3.7 MPa (at 40 at.% burnup). Since the yield stress of the cladding (Al-1060) is known as about 28 MPa at room temperature[5], the hoop stress of 3.7 MPa seems to be well below the yield stress, although the yield stress will decrease to a lower value in the temperature range of 410 K-440 K.

3.4. Burnup Effect on Fuel Deformation

Fig. 9 shows the variation of the maximum hoop stress with element burnup. The maximum hoop stress is the hoop stress at cladding outer surface. Fig. 9 illustrates that the maximum hoop stress at each burnup is 3-5 MPa in the whole burnup range. As indicated in the power-law creep equation (9), the stress at cladding is determined by the creep rate and temperature. As discussed in the section 3.2, the creep strain rate of cladding is almost determined by

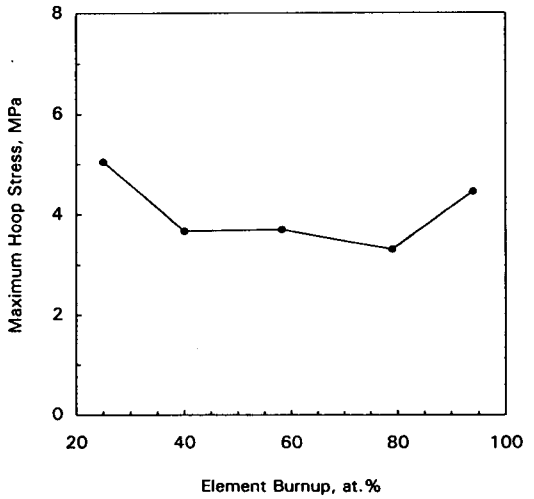

Fig. 9. Variation of the Maximum Hoop Stress with Element Burnup

the swelling strain rate of fuel meat, therefore the stress at cladding is determined by the swelling of fuel meat and the temperature of cladding. From the Fig. 9, we can also derive an important conclusion that the maximum hoop stress (3-5 MPa) in the cladding of HANARO fuel is believed to be well below the yield stress of cladding under normal operation conditions.

The variations of hoop strain at cladding outer surface and the element volume change are illustrated in Fig. 10, as the functions of the element burnup. The hoop strain increases to about 0.045 (4.5%) with increasing the burnup to about 80 at.%, and after then it slightly decreases. The small decrease in the hoop strain after 80 at.% may be resulted from the small swelling due to relatively low element power of 34.7 kW/m (see Table 2). The volume expansion of element also has similar trend, in which a peak volume change of about 9.2% is predicted for this HANARO fuel at 80 at.% burnup.

3.5. Comparison of Element Volume Changes

Fig. 11 compares the calculated volume change with the measured volume change of experiment FZZ-918[1, 2]. In this experiment the volume change of fuel (mini-elements) was measured on the cold fuel, therefore, the present simulation also extracted the portion of thermal expansion from the total volume change of hot fuel. In order to calculate the volume change of cold fuel, 7 cases (case 2 to case 8) were simulated for NRU fuel.

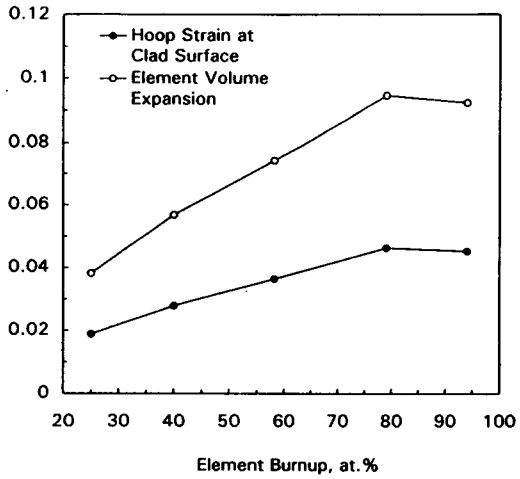

Fig. 10. Variations of Hoop Strain and Volume Expansion of Element with Element Burnup

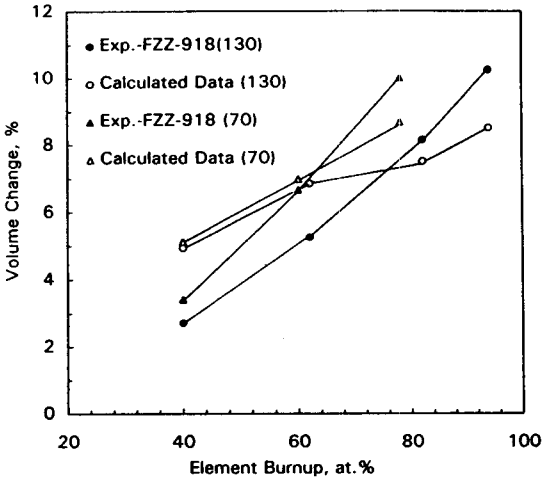

Fig. 11. Comparison of Calculated Data with Measured Data (FZZ-918); the Numbers in the Parenthesis (130 and 70) Mean Average Uranium-Silicide Particle Size

Fig. 11 shows that both the calculated data and the measured data increase with burnup in a similar manner. However, the slopes of the curves are different from each other; the calculated data are larger than the measured data at small burnups, but become smaller at large burnups. During deformation the cladding does not change its volume because the constant volume condition is applied, so the volume change measured or calculated on the fuel surface is totally caused by the swelling of fuel meat. So it seems that the swelling model[4] over-estimates the fuel swelling at small burnups and under-estimates it at large burnups.

4. Summary and Conclusions

A deformation model, STRESS, was developed to simulate the deformation behaviour of uranium-sili-

cide dispersion fuel during normal and off-normal operation conditions. The STRESS model has a capability of calculating the stress distribution, strain distribution, strain rate distribution etc. Through the sample calculations, the STRESS model was judged to calculate successfully deformation of the uranium- silicide dispersion fuels.

For the calculation results for a HANARO fuel element, the important points are summarized as follows : The major deformation mechanisms of the uranium-sicilide dispersion fuel are the swelling of fuel meat and the creep of cladding. Most of the swelling strain of fuel meat is transformed into the creep strain of cladding at fuel meat-cladding interface. The maximum hoop stress predicted at cladding outer surface is believed to be well below the yield stress of the cladding ; the maximum hoop stress does not exceed about 5 MPa in the whole burnup range.

For both fuel designs considered, the predicted volume change of the element does not exceed 10% in the whole burnup range up to 94 at.%. Comparison of the calculated volume change and the measured volume change of experiment FZZ-918 showed that the swelling model over-estimates the fuel swelling at small burnups and under-estimates it at large burnups.

References

1. D.F. Sears. et. al., "Fabrication and Irradiation Testing of LEU Fuels at CRNL : Status as of 1987 September," Proceedings of International Meeting on Reduced Enrichment for Research and Test Reactors, Buenos Aires, September 28-October 2 (1987)
2. D.F. Sears, et. al., Status of LEU Fuel 1Develop ment and Conversion of NRU, Proceedings of International Meeting on Reduced Enrichment for Research and Test Reactors, Berin, Germany, September 10~14 (1989)
3. 국일현외 다수, KMRR 핵연료개발, 연구보고서 KAERI/RR-1131/91 (1991)
4. W. Hwang, A Comprehensive Swelling Model of Silicide Dispersion Fuel for Research Reactor, Journal of Korean Nuclear Society, Vol. 24, pp. 40~51 (1992)
5. ASM Metals Handbook, Vol. 2-Properties and Selections of Nonferrous Alloys and Pure Metals, 8th Edition, pp. 64.
6. P.C.R. Cunha and H.J. Kestenbach, Metalurgia-ABM, Vol. 35, pp. 257 (1979)
7. J.E. Dorn, Creep and Recovery, American Society for Metals (1957)
8. D.R. Olander, Fundamental Aspects of Nuclear Reactor Fuel Elements, Chapter 21 (1976)
9. M.A. Meyers and K.K. Chawla, Mechanical Metallurgy, Chapter 20, Prentice-Hall Inc (1984)
10. 강영하외 3명, 고체역학의 기초와 응용, 동명사, (1980)